


Bearing fault diagnosis of wind turbine based on intrinsic time-scale decomposition frequency spectrum

Proc IMechE Part O:
J Risk and Reliability
2014, Vol. 228(6) 558–566
© IMechE 2014
Reprints and permissions:
sagepub.co.uk/journalsPermissions.nav
DOI: 10.1177/1748006X14539678
pio.sagepub.com


Xueli An¹ and Dongxiang Jiang²

Abstract

In order to better identify the complex running conditions of wind turbine main bearings, we developed a bearing fault diagnosis method based on intrinsic time-scale decomposition frequency spectrum. The main bearing acceleration vibration signal from wind turbine is captured under four conditions—good bearing, outer race fault, inner race fault and roller fault. The proposed method consists of the following steps. First, the main bearing acceleration vibration signal is decomposed into several proper rotation components by using the intrinsic time-scale decomposition method. Second, the frequency spectrum of the first few proper rotation components (containing dominant fault features) is analyzed. The dominant resonant frequency range of each analyzed rotation component is derived, and then, the sum of frequency amplitude in said frequency range can be obtained. This sum is regarded as the fault feature vectors. Finally, the fault feature vectors are input to the least square support vectors machine, and the faults of wind turbine main bearing then can be diagnosed. The experiment results show that the proposed method can diagnose failures of wind turbine bearings quickly and more accurately.

Keywords

Intrinsic time-scale decomposition, frequency spectrum, frequency range, least square support vector machine, wind turbine, spherical roller bearing, fault diagnosis

Date received: 6 December 2013; accepted: 20 May 2014

Introduction

Most wind farms are located in regions with harsh environment that are often under extreme weather conditions. The components of wind turbine would gradually age, and failures would become frequent with the increase in total running time. As a result, it is essential to monitor and analyze the conditions of wind turbine in order to ensure their safety and stability, and to detect and diagnose their faults in time.^{1–6} Bearings are widely used in main shafts, yaws, pitches, generators, gearboxes and many other parts of wind turbines. Faults of bearing, which are complex, nonlinear, time-varying and multi-coupling, make up the majority of wind turbine failures.^{7,8}

Some works have been done about the fault diagnosis of wind turbines.^{8–13} An et al.⁸ put forward a fault diagnosis method of wind turbine bearing based on intrinsic time-scale decomposition (ITD). In the reference, main bearing's vibration signal is decomposed into several proper rotation components by the ITD method. The frequency centers of the proper rotation

components are computed and considered as fault feature vectors to diagnose the wind turbine bearing faults. Liu et al.⁹ proposed a wind turbine fault diagnosis method based on the local mean decomposition (LMD) technology. LMD is an iterative approach to demodulate amplitude and frequency modulated signals, which makes it suitable for obtaining the instantaneous frequencies of wind turbine vibration signals. Jiang et al.¹⁰ presented a denoising method based on adaptive Morlet wavelet and singular value decomposition to extract the features of wind turbine vibration signals. The results of experiment analysis show that the method

¹China Institute of Water Resources and Hydropower Research, Beijing, China

²State Key Laboratory of Control and Simulation of Power System and Generation Equipments, Department of Thermal Engineering, Tsinghua University, Beijing, China

Corresponding author:

Xueli An, China Institute of Water Resources and Hydropower Research, Haidian District, Beijing 100038, China.
Email: an_xueli@163.com

has better denoising performance than other wavelet transforms. Bennouna et al.¹¹ presented a linear and nonlinear system based on polynomial approximation for the doubly fed induction generator (DFIG) of a wind turbine at variable speed. It uses fault signature analysis to detect the biases in the system. Tang et al.¹² presented a fault diagnosis method based on Morlet wavelet transformation and Wigner–Ville distribution (WVD). Morlet wavelet is used to remove the noise in raw vibration signals, and auto terms window function is used to suppress the cross terms in WVD. This method can effectively suppress the cross terms and extract the fault features. Feng et al.¹³ integrated ensemble empirical mode decomposition (EEMD) and energy separation for amplitude and frequency demodulations of wind turbine planetary gearbox vibration signals. EEMD is used to decompose the complex signal into mono-components. The energy separation method is used to estimate the instantaneous envelope and frequency of the decomposed components. This method can detect and locate the wear and chipping faults from a sun gear of the planetary gearbox test rig.

Frei and Osorio¹⁴ presented the ITD method in 2006. This method can decompose a complex signal into several proper rotation components and a trend component. It can accurately extract the dynamic features of nonstationary signals and has a higher decomposition efficiency and frequency resolution. The method is suitable for analyzing time-varying, nonstationary signals. As it does not involve spline interpolation and screening process, it has low edge effect and can be used to handle large amounts of real-time data.

ITD, empirical mode decomposition (EMD)¹⁵ and EEMD¹⁶ are all self-adaptive signal decomposition methods. However, as it has no need for a sifting process, the ITD method has higher computational efficiency than EMD and EEMD. Wavelet transform¹⁷ also can be used to decompose a complicated signal into a number of components. However, the wavelet base function and decomposition scales need to be defined at first. That is to say the wavelet method is nonadaptive in nature. Due to its advantages in adaptability and higher computing efficiency, the ITD method is well suitable for application of real-time signal analysis.

The ITD provides good analysis of nonstationary, nonlinear signal at high speed. At the same time, the least square support vector machine (LS-SVM) has strong capacity for approximation and generalization and fast learning speed.^{18–21} Therefore, a wind turbine's spherical roller bearing fault diagnosis model based on ITD frequency spectrum and the LS-SVM is presented. This may provide a new way for the online diagnosis of the wind turbines.

ITD

The ITD^{8,14} method decomposes a vibration signal into a series of proper rotation components and a trend component. The instantaneous amplitude and

frequency of the proper rotation components are analyzed in the frequency spectrum. Through analyzing the spectrum, the amplitude and frequency modulation of the vibration signal can be obtained, respectively. For the signal X_t , ξ is defined as the baseline extraction operator. After extracting a baseline from the signal X_t , the rest of the signal becomes an inherent rotation. The first decomposition of X_t is as follows¹⁴

$$X_t = \xi X_t + (1 - \xi)X_t = L_t + H_t \quad (1)$$

where $L_t = \xi X_t$ is the baseline signal and $H_t = (1 - \xi)X_t$ is the proper rotation component.

Assuming $\{\tau_k, k = 1, 2, \dots\}$ is the time index of the local extrema values of X_t , let $\tau_0 = 0$. For simplicity, $X(\tau_k)$ and $L(\tau_k)$ are expressed by using X_k and L_k , respectively. It is assumed that L_t and H_t are defined in $[0, \tau_k]$, and X_t is defined in $t \in [0, \tau_{k+2}]$. The subsection linearity baseline extraction operator, ξ , then can be defined in contiguous extrema interval $(\tau_k, \tau_{k+1}]$

$$\xi X_t = L_t = L_k + \left(\frac{L_{k+1} - L_k}{X_{k+1} - X_k} \right) (X_t - X_k) \quad (2)$$

In equation (2), L_{k+1} can be expressed as

$$L_{k+1} = \alpha \left[X_k + \left(\frac{\tau_{k+1} - \tau_k}{\tau_{k+2} - \tau_k} \right) (X_{k+2} - X_k) \right] + (1 - \alpha)X_{k+1} \quad (3)$$

where $\alpha \in (0, 1)$, usually $\alpha = 0.5$. Decomposition can extract a baseline signal and a proper rotation component, the latter denoting the local relative high frequency of the decomposed signal. Taking the baseline signal as the input signal, the decomposition is continued until a monotone signal is obtained. Using this method, the original signal is decomposed into several proper rotation components of frequency ranges from high to low and a monotone trend component. The whole process can be expressed as

$$\begin{aligned} X_t &= \psi X_t + \xi X_t = \psi X_t + (\psi + \xi)\xi X_t \\ &= [\psi(1 + \xi) + \xi^2]X_t \\ &= \left(\psi \sum_{k=0}^{p-1} \xi^k + \xi^p \right) X_t \end{aligned} \quad (4)$$

where $\psi \xi^k X_t$ is the $(k + 1)$ th layer of the proper rotation and $\xi^p X_t$ is a monotone trend or an extracted lowest frequency baseline when the decomposition is stopped before the monotone trend is obtained.

The decomposed components from the ITD method have certain physical meanings. They can effectively reflect the characteristics of the original signal and are suitable for analyzing the amplitude and frequency modulation of the signal. In this article, the vibration signal of spherical roller bearing fault in wind turbine is decomposed using the ITD algorithm. The instantaneous amplitudes of main components are extracted and are analyzed in frequency spectrum. And this can

Table 1. Definitions of frequency ranges for the ITD decomposed results of vibration signals under four conditions.

Operation condition	The frequency range of dominant spectral peak					
	c_1	c_2	c_3	c_4	...	c_n
Normal condition	$[\alpha_1, \alpha_2]$	$[\alpha_3, \alpha_4]$	$[\alpha_5, \alpha_6]$	$[\alpha_7, \alpha_8]$...	$[\alpha_{2n-1}, \alpha_{2n}]$
Outer race fault	$[\beta_1, \beta_2]$	$[\beta_3, \beta_4]$	$[\beta_5, \beta_6]$	$[\beta_7, \beta_8]$...	$[\beta_{2n-1}, \beta_{2n}]$
Inner race fault	$[\gamma_1, \gamma_2]$	$[\gamma_3, \gamma_4]$	$[\gamma_5, \gamma_6]$	$[\gamma_7, \gamma_8]$...	$[\gamma_{2n-1}, \gamma_{2n}]$
Roller fault	$[\delta_1, \delta_2]$	$[\delta_3, \delta_4]$	$[\delta_5, \delta_6]$	$[\delta_7, \delta_8]$...	$[\delta_{2n-1}, \delta_{2n}]$

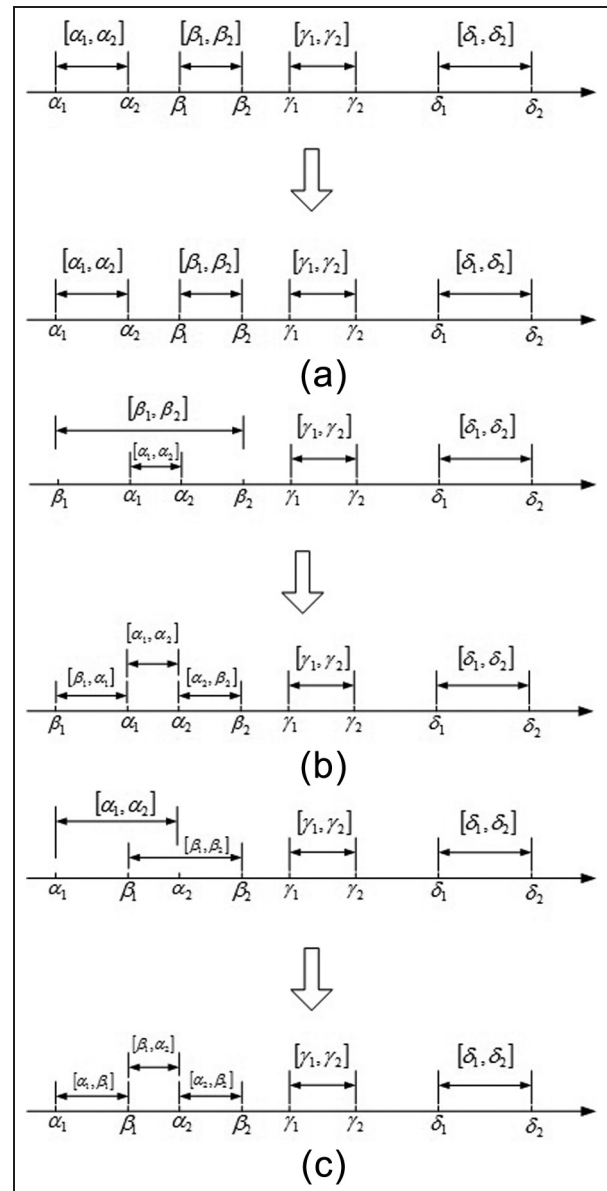
get the bearing failure characteristics of the wind turbine.

Bearing fault diagnosis for wind turbine based on ITD frequency spectrum

The wind condition in a wind farm is highly unstable, and the faults of spherical roller bearing are random and nonlinear. Therefore, when the roller bearing failure occurs, the vibration signal has a complex modulated composition. For the purpose of extracting the bearing fault feature, the vibration signal should be demodulated effectively. In this article, the ITD method is adopted to effectively decompose the vibration acceleration signal of bearing fault. The signal is decomposed into a series of proper rotation components, c_1, c_2, \dots, c_n . The frequency spectrum of the proper rotation components, c_i , which contains an obvious impact feature, is analyzed to extract the bearing fault feature. That is, when the roller bearing of the wind turbine goes wrong in inner race, outer race, roller or other parts, an impact signal will be generated. The spectral peak of natural frequencies in the frequency spectrum of proper rotation component, c_i , will appear. The dominant spectral peak frequency range of c_i is different when the roller bearing is in normal condition, or experiencing a fault in outer race, inner race or roller. See the list in Table 1.

Based on an overall analysis of the four conditions, the dominant spectral peak frequency ranges of c_1 are defined as follows: (1) If $[\alpha_1, \alpha_2]$, $[\beta_1, \beta_2]$, $[\gamma_1, \gamma_2]$ and $[\delta_1, \delta_2]$ are independent of each other, then the peak frequency range is $\{[\alpha_1, \alpha_2], [\beta_1, \beta_2], [\gamma_1, \gamma_2], [\delta_1, \delta_2]\}$, as shown in Figure 1(a); (2) if $[\alpha_1, \alpha_2] \subset [\beta_1, \beta_2]$, and $[\beta_1, \beta_2]$, $[\gamma_1, \gamma_2]$ and $[\delta_1, \delta_2]$ are independent of each other, then the peak frequency range is $\{[\beta_1, \alpha_1], [\alpha_1, \alpha_2], [\alpha_2, \beta_2], [\gamma_1, \gamma_2], [\delta_1, \delta_2]\}$, as shown in Figure 1(b), and otherwise similar to other cases; (3) if $[\alpha_1, \alpha_2] \cap [\beta_1, \beta_2] = [\theta_1, \theta_2]$, they and $[\gamma_1, \gamma_2]$, $[\delta_1, \delta_2]$ are independent of each other, then the peak frequency range is $\{[\alpha_1, \beta_1], [\beta_1, \alpha_2], [\alpha_2, \beta_2], [\gamma_1, \gamma_2], [\delta_1, \delta_2]\}$, as shown in Figure 1(c) and so on. The definition of spectral peak frequency ranges of c_2, \dots, c_n is similar to c_1 .

If the spectral peak frequency ranges of c_1 are $\{[\alpha_1, \alpha_2], [\beta_1, \beta_2], [\gamma_1, \gamma_2], [\delta_1, \delta_2]\}$, then the fault feature vector of c_1 is defined as $\{\sum_{f=\alpha_1}^{\alpha_2} s_1(f), \sum_{f=\beta_1}^{\beta_2} s_1(f), \sum_{f=\gamma_1}^{\gamma_2} s_1(f), \sum_{f=\delta_1}^{\delta_2} s_1(f)\}$, where $s_1(f)$ is the frequency

**Figure 1.** Selecting the dominant spectral peak frequency ranges: (a) Case 1, (b) Case 2 and (c) Case 3.

spectrum of c_1 and $f = 1, \dots, 1000$ is the frequency value of the frequency spectrum. The definition of fault feature vectors of c_2, \dots, c_n is similar to c_1 .

The ITD decomposes the vibration signal into several proper rotation components with frequencies from high to low, and the fault feature of roller bearing is

mainly in the high-frequency part. So, the running condition of wind turbine main bearing can be identified by using the LS-SVM to analyze the fault feature vectors of the first few rotation components. The fault diagnosis method of wind turbine spherical roller bearings is developed, and the detailed steps are as follows:

1. At laboratory scale, four experiments of the direct-drive wind turbine with a main shaft supported by two spherical roller bearings are carried out. These experiments include the conditions of the normal operation, outer race fault, inner race fault and roller fault of spherical roller bearing. The bearing vibration acceleration signals are selected as the sample data.
2. The sample data are decomposed using the ITD method into a series of proper rotation components, c_1, c_2, \dots, c_n . They have different characteristic scales.
3. The first several proper rotation components with obvious impact elements are analyzed in frequency spectrum. The extracted bearing fault feature A can be expressed as: $A = \{\sum_{f=\alpha_1}^{\alpha_2} s_1(f), \sum_{f=\beta_1}^{\beta_2} s_1(f), \sum_{f=\gamma_1}^{\gamma_2} s_1(f), \sum_{f=\delta_1}^{\delta_2} s_1(f), \dots, \sum s_2(f), \dots, \sum s_n(f), \dots\}$.
4. The feature vectors A are input to LS-SVM for training.
5. The test samples are identified based on the trained LS-SVM.

Case study

The ability of the presented method to identify faults is verified with a complete experimental case. The experimental setup of direct-drive wind turbine is displayed in Figure 2. This system consists of a wind tunnel, a wind wheel, a main shaft, main bearings and a generator. The generator is a three-phase permanent magnet alternating current (AC) synchronous generator, rated power: 300 W and rated speed: 400 r/min. The main shaft is supported at its ends by two spherical roller bearings. The test bearing (good condition, or with outer race fault, inner race fault or roller fault) is closer to the wind wheel. The other bearing at the farther end is assumed to be free from faults. The main shaft and generator are connected by flexible coupling. In the system, the wind is produced by a wind tunnel under laboratory conditions. In order to produce different wind speeds, the axial fan of 15 kW is adjusted by an inverter. When the turbine blades capture wind energy from wind tunnel and start moving, the main shaft, which is connected to the generator, is driven to spin to generate AC electricity. The rectifier is used to convert the generator's AC output to direct current (DC). It is stored in the batteries connected to the rectifier. When the batteries are fully charged, the generator's output is transmitted into the inverter to supply a 220-V AC load. A test system is developed to monitor the wind

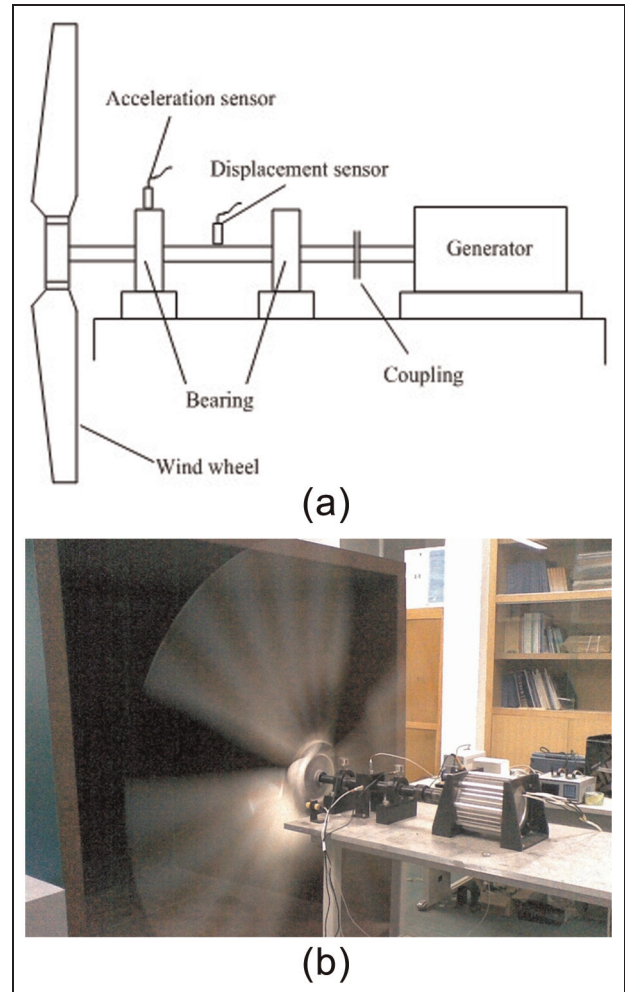


Figure 2. Test stand of direct-drive wind turbine: (a) test stand schematic diagram and (b) test stand picture.

turbine's operation condition. The sampling rate is 2000 Hz, and the sampling length is 8192 points for all conditions. The vibration signals of the main bearing are obtained by an acceleration sensor mounted on top of the test bearing pedestal. The vibration signals of the main shaft are picked up by two displacement sensors installed horizontally and vertically at the center of main shaft between two bearings. In the following analysis, four experiments under conditions of normal operation, outer race fault, inner race fault and roller fault are carried out. The bearing faults of spherical roller bearings are set by grooving using a linear cutting method. The slot width is 0.2 mm and the slot depth is 0.3 mm, as shown in Figure 3. The faulty bearings are installed in the near wind wheel. The rotating frequency of wind turbine is 4.33 Hz in these experiments.

The vibration acceleration signals of wind turbine main bearing under conditions of normal operation, outer race fault, inner race fault and roller fault are shown in Figure 4. It can be seen from Figure 4 that the vibration signals in the four conditions are highly complex. The bearing conditions cannot be readily identified from Figure 4. The ITD method is used to

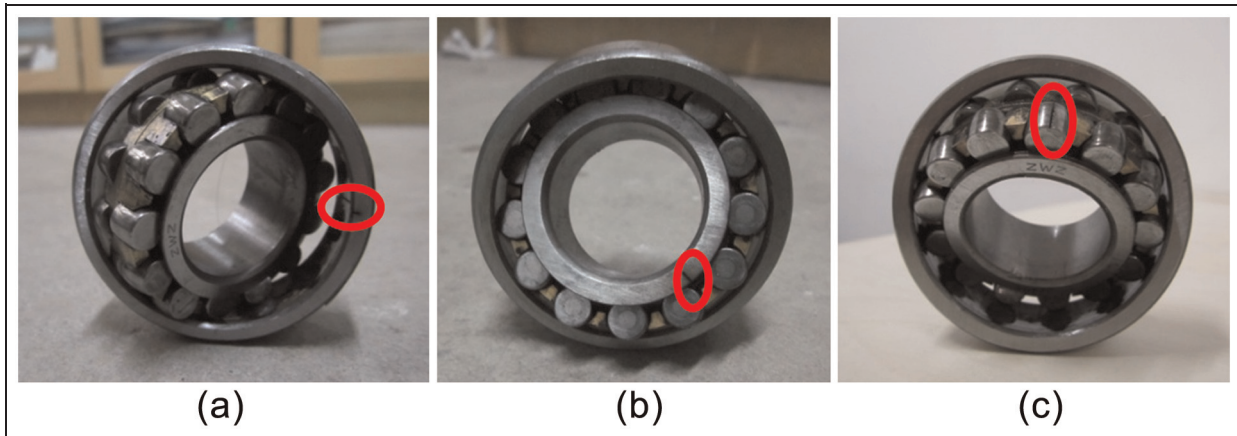


Figure 3. Faults in the spherical roller bearing: (a) outer race fault, (b) inner race fault and (c) roller fault.

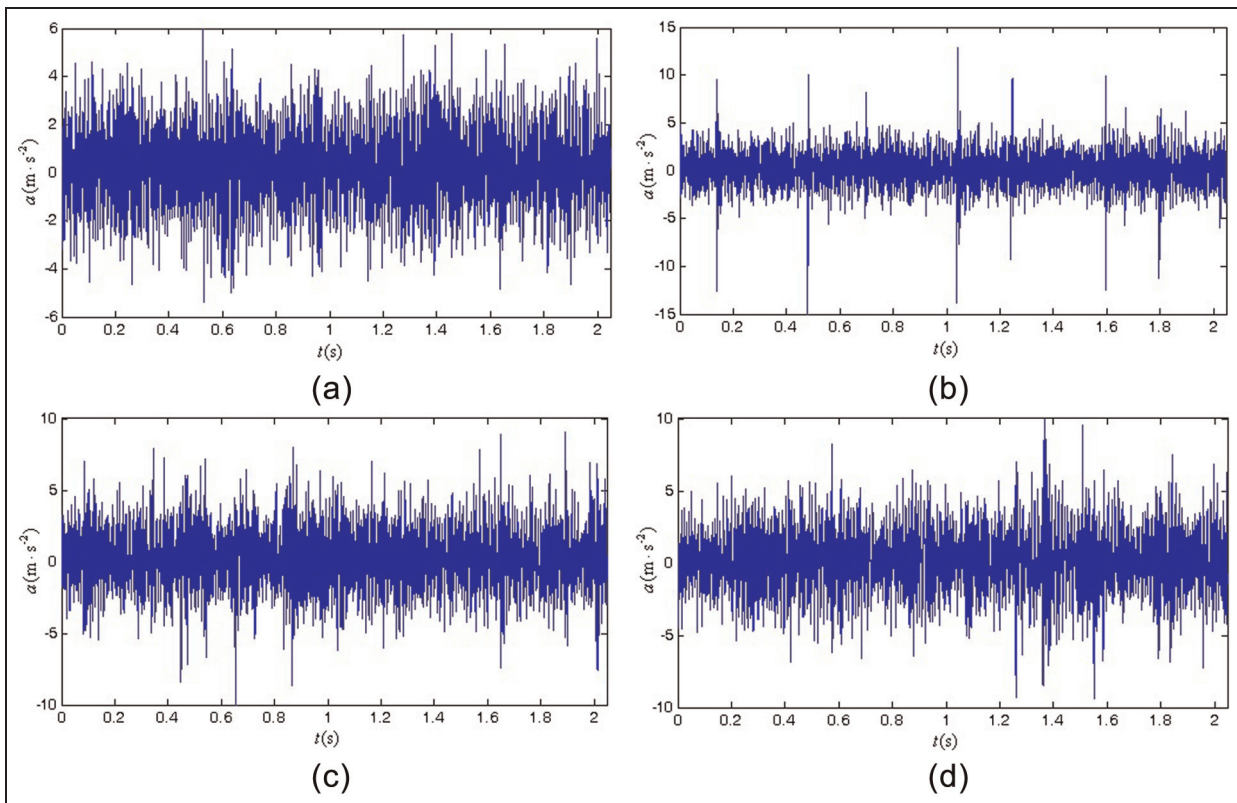


Figure 4. Time domain waveform of main bearing vibration acceleration signals in four conditions: (a) normal condition, (b) outer race fault, (c) inner race fault and (d) roller fault.

decompose these vibration signals and obtain the corresponding proper rotation components. Because of the limited paper space, only the first four components (including dominant fault information) are given in Figure 5. It can be seen from Figure 5 that the ITD method had decomposed the vibration signal into a number of proper rotation components with different time scales. And this can improve the frequency resolution of the decomposed signal.

Figure 6 is the frequency spectrum of proper rotation components of vibration acceleration signal in four

conditions. From these figures, it can be seen that the spectra under different condition are obviously different. Figure 6(a) shows when wind turbine main bearing is in normal operation, the peaks are primarily in [450 Hz, 550 Hz] for the first proper rotation component c_1 . For the second proper rotation component c_2 , there are significant peaks in [150 Hz, 250 Hz]. For the third proper rotation component c_3 , the peaks in [60 Hz, 100 Hz] are dominant. And the peaks cover the main positions in [1 Hz, 50 Hz] for the fourth proper rotation component c_4 .

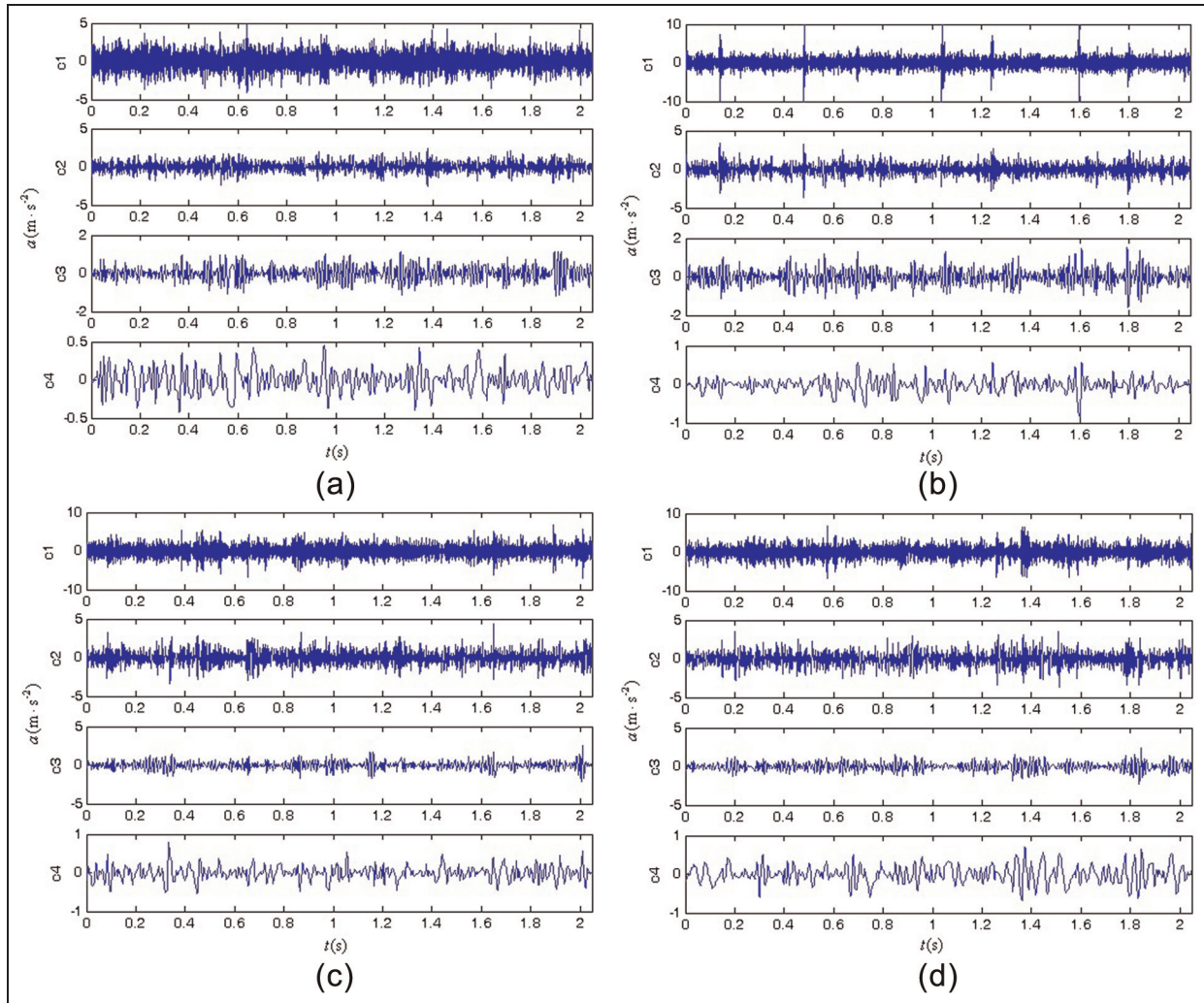


Figure 5. The ITD decomposed results of main bearing vibration acceleration signals in four conditions: (a) normal condition, (b) outer race fault, (c) inner race fault and (d) roller fault.

It can be seen from Figure 6(b) that when the outer race fault of wind turbine main bearing occurs, the peaks in [700 Hz, 1000 Hz] of c_1 , [150 Hz, 250 Hz] of c_2 , [60 Hz, 100 Hz] of c_3 and [1 Hz, 50 Hz] of c_4 are obvious. In Figure 6(c), when the inner race fault of wind turbine main bearing occurs, for c_1 , c_2 , c_3 and c_4 , there are dominant peaks in [700 Hz, 1000 Hz], [150 Hz, 250 Hz], [60 Hz, 100 Hz] and [1 Hz, 50 Hz], respectively. In Figure 6(d), when the roller fault occurs, the peaks in [300 Hz, 450 Hz], [50 Hz, 100 Hz], [60 Hz, 100 Hz] and [1 Hz, 50 Hz] are dominant for c_1 , c_2 , c_3 and c_4 , respectively.

Therefore, based on an overall analysis of the four conditions of the main bearing, the feature frequency ranges of c_1 can be obtained, expressed as [300 Hz, 450 Hz], [450 Hz, 550 Hz] and [700 Hz, 1000 Hz]; the feature frequency range of c_2 can be expressed as [50 Hz, 100 Hz] and [150 Hz, 250 Hz]; the feature frequency range of c_3 is [60 Hz, 100 Hz] and the feature frequency range of c_4 is [1 Hz, 50 Hz]. The fault feature vectors of wind turbine main bearing based on the feature frequency ranges of c_1 – c_4 are denoted by $A = A_1, A_2,$

$A_3, A_4, A_5, A_6, A_7 = \{\sum_{f=300}^{450} s_1(f), \sum_{f=450}^{550} s_1(f), \sum_{f=700}^{1000} s_1(f), \sum_{f=50}^{100} s_2(f), \sum_{f=150}^{250} s_2(f), \sum_{f=60}^{100} s_3(f), \sum_{f=1}^{50} s_4(f)\}$, where $s_1(f)$ is the frequency spectrum of the first proper rotation component c_1 , $s_2(f)$ is the frequency spectrum of the second proper rotation component c_2 , $s_3(f)$ is the frequency spectrum of the third proper rotation component c_3 , $s_4(f)$ is the frequency spectrum of the fourth proper rotation component c_4 and $f = 1, \dots, 1000$ is the frequency value for the frequency spectrum. The fault feature vector A in the four patterns (bearing in normal operation, outer race fault, inner race fault and roller fault), respectively, are taken as inputs for the LS-SVM classifiers.

The vibration acceleration signals of wind turbine main bearing in four conditions (normal running, outer race fault, inner race fault and roller fault) are collected. For each condition, 40 sets of data are selected randomly, 4×40 sets of data in total. For the 160 sets of data, 40 sets of data (10 sets for each condition) are chosen as standard samples to compute the fault feature vectors $A = A_1, A_2, A_3, A_4, A_5, A_6, A_7 =$

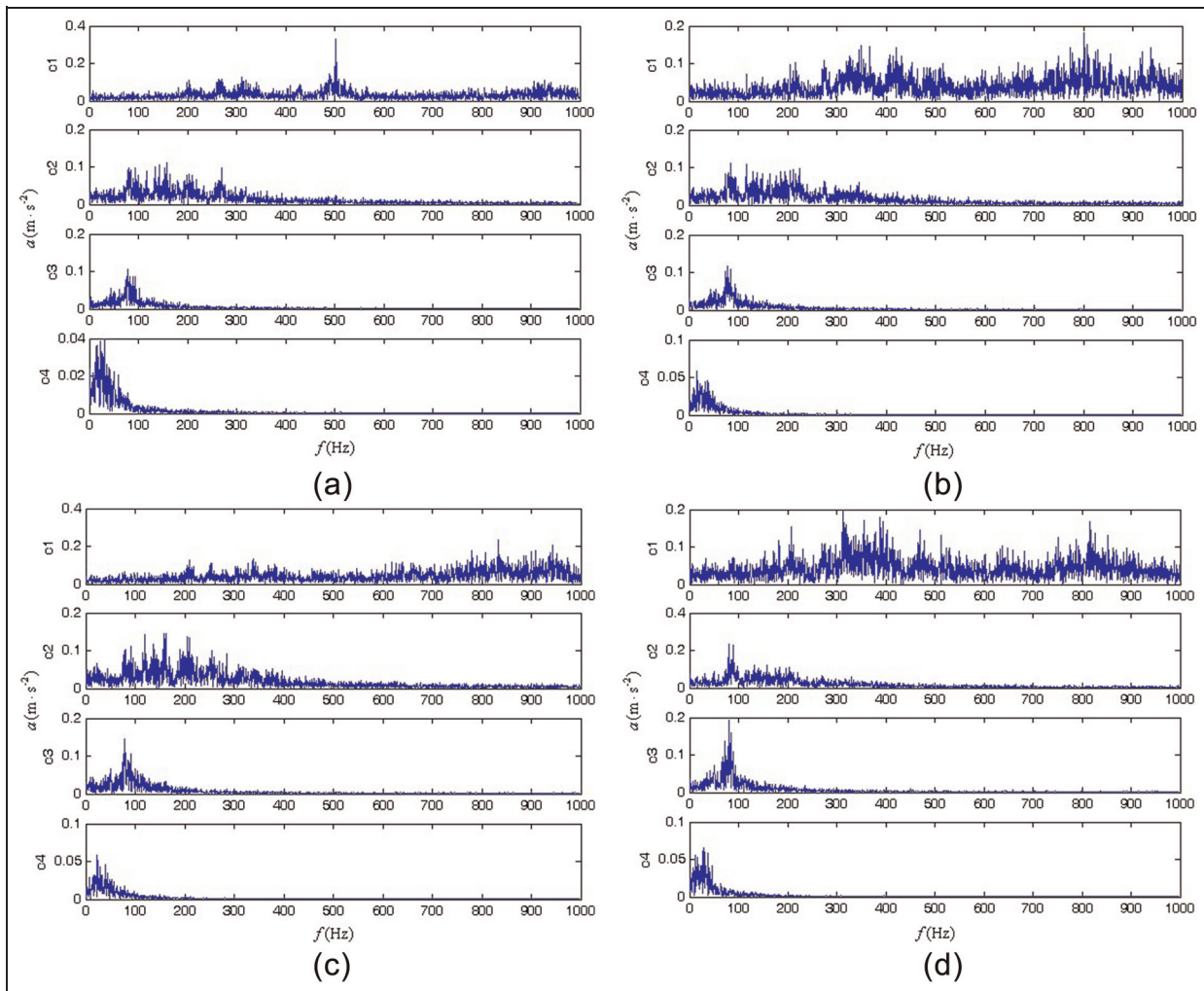


Figure 6. The spectra of the ITD decomposed results of acceleration signals under four conditions: (a) normal condition, (b) outer race fault, (c) inner race fault and (d) roller fault.

$\{\sum_{f=300}^{450} s_1(f), \sum_{f=450}^{550} s_1(f), \sum_{f=700}^{1000} s_1(f), \sum_{f=50}^{100} s_2(f), \sum_{f=150}^{250} s_2(f), \sum_{f=60}^{100} s_3(f), \sum_{f=1}^{50} s_4(f)\}$. The computed fault feature vectors A are input to the LS-SVM classifier to train it. And as the test samples, the remaining 120 sets of data were tested. The main bearing condition is classified by the output of the LS-SVM classifier. The identification accuracy ratio of test samples is 100%. Due to limited space, Table 2 only gives 20 test samples with four conditions based on the first four proper rotation components decomposed by ITD methods.

In Table 2, the A_1 , A_2 and A_3 are the amplitude summations in frequency ranges [300 Hz, 450 Hz], [450 Hz, 550 Hz] and [700 Hz, 1000 Hz], respectively, of the first proper rotation component c_1 . In other words, $A_1 = \sum_{f=300}^{450} s_1(f)$, $A_2 = \sum_{f=450}^{550} s_1(f)$ and $A_3 = \sum_{f=700}^{1000} s_1(f)$, where $s_1(f)$ is the frequency spectrum of the first proper rotation component c_1 and $f = 1, \dots, 1000$ is the frequency value for the frequency spectrum. A_4 and A_5 are the amplitude summation in frequency ranges [50 Hz, 100 Hz] and [150 Hz, 250 Hz], respectively, of the second proper rotation component

c_2 . Namely, $A_4 = \sum_{f=50}^{100} s_2(f)$ and $A_5 = \sum_{f=150}^{250} s_2(f)$, where $s_2(f)$ is the frequency spectrum of the second proper rotation component c_2 and $f = 1, \dots, 1000$ is the frequency value for the frequency spectrum. A_6 is the amplitude summation in frequency range [60 Hz, 100 Hz] of the third proper rotation component c_3 . That is, $A_6 = \sum_{f=60}^{100} s_3(f)$, where $s_3(f)$ is the frequency spectrum of the third proper rotation component c_3 and $f = 1, \dots, 1000$ is the frequency value for the frequency spectrum. A_7 is the amplitude summation in frequency range [1 Hz, 50 Hz] of the fourth proper rotation component c_4 . Accordingly, $A_7 = \sum_{f=1}^{50} s_4(f)$, where $s_4(f)$ is the frequency spectrum of the fourth proper rotation component c_4 and $f = 1, \dots, 1000$ is the frequency value for the frequency spectrum.

Conclusion

To handle the nonstationary and nonlinear vibration signal of the wind turbine bearing fault, a fault diagnosis method of the wind turbine bearing based on ITD frequency spectrum and LS-SVM is proposed. First,

Table 2. Main bearing fault feature of wind turbine based on the spectrum of the ITD decomposed results of vibration signals.

No.	Main bearing condition	Main bearing fault feature						
		A ₁	A ₂	A ₃	A ₄	A ₅	A ₆	A ₇
1	Normal	9.94	10.23	19.61	3.81	6.04	3.19	1.57
2		9.92	10.48	20.68	3.21	6.26	3.09	1.45
3		10.4	10.16	20.58	3.11	6.79	3.28	1.68
4		9.75	9.61	20.07	3.66	6.38	2.75	1.79
5		10.73	10.66	20.21	3.98	6.76	2.89	1.65
6	Outer race fault	12.63	7.08	32.43	5.71	7.54	4.71	2.38
7		17.27	8.8	33.46	6.18	8.29	4.3	2.29
8		19.36	9.23	31.92	5.74	8.86	4.33	2.21
9		18.37	8.79	30.21	4.3	7.71	3.77	1.95
10		18.99	10.62	29.82	4.38	7.51	3.67	2.09
11	Inner race fault	13.38	7.97	38.01	4.06	8.62	3.59	2.21
12		12.45	7.41	36.78	3.92	9.03	3.66	1.89
13		12.22	7.01	36.03	4.01	8.7	3.98	2.14
14		12.69	6.95	36.76	3.61	8.72	3.43	1.88
15		11.8	7.25	38.36	3.22	9.27	3.71	2.01
16	Roller fault	18.05	8.81	22.37	5.51	8.08	4.01	2.34
17		18.17	8.67	23.3	5.84	7.33	3.76	2.12
18		19.45	8.61	24.25	5.84	8.13	3.76	2.75
19		18.68	8.61	21.68	5.28	7.9	3.87	2.13
20		18.85	8.89	24.12	5.42	7.31	3.93	2.06

using the ITD method, a complex vibration signal is decomposed into several proper rotation components. The decomposed components can effectively reflect the characteristics of the original signal. Then, the first few proper rotation components (containing dominant fault features) are analyzed in their frequency spectra, which turn out to be of great impact. The sum of frequency amplitudes in frequency ranges containing fault characteristics is computed as the bearing fault feature vectors. Finally, the LS-SVM is used as a classifier to train and identify the running condition of the wind turbine bearings. Experiment results show that the proposed method is effective in identifying the wind turbine bearing faults.

Declaration of conflicting interests

The authors declare that there is no conflict of interest.

Funding

This work was supported by the National Natural Science Foundation of China (grant numbers 51174273 and 51309258).

References

- Hameed Z, Hong Y, Cho Y, et al. Condition monitoring and fault detection of wind turbines and related algorithms: a review. *Renew Sust Energ Rev* 2009; 13(1): 1–39.
- Amirat Y, Benbouzid M, Al-Ahmar E, et al. A brief status on condition monitoring and fault diagnosis in wind energy conversion systems. *Renew Sust Energ Rev* 2009; 13(9): 2629–2636.
- An X and Jiang D. Correlation analysis of oil temperature trend for wind turbine gearbox. In: *Proceedings of the ASME 2010 international design engineering technical conferences & computers and information in engineering conference*, Montreal, QC, Canada, August 15–18, 2010, pp.719–722. New York: ASME.
- Barszcz T and Randall R. Application of spectral kurtosis for detection of a tooth crack in the planetary gear of a wind turbine. *Mech Syst Signal Pr* 2009; 23(4): 1352–1365.
- An X and Jiang D. Chaotic characteristics identification and trend prediction of running state for wind turbine. *Electr Power Automat Equip* 2010; 30(3): 15–19.
- Hameed Z and Vatn J. Role of grouping in the development of an overall maintenance optimization framework for offshore wind turbines. *Proc IMechE, Part O: J Risk and Reliability* 2012; 226(6): 584–601.
- Zhao M. *Fault feature analysis and experimental investigation for wind turbine*. Thesis for the Degree of Master of Engineering, Tsinghua University, Beijing, China, 2010.
- An X, Jiang D, Chen J, et al. Application of the intrinsic time-scale decomposition method to fault diagnosis of wind turbine bearing. *J Vib Control* 2012; 18(2): 240–245.
- Liu W, Zhang W, Han J, et al. A new wind turbine fault diagnosis method based on the local mean decomposition. *Renew Energ* 2012; 48: 411–415.
- Jiang Y, Tang B, Qin Y, et al. Feature extraction method of wind turbine based on adaptive Morlet wavelet and SVD. *Renew Energ* 2011; 36(8): 2146–2153.
- Bennouna O, Heraud N, Camblong H, et al. Diagnosis and fault signature analysis of a wind turbine at a variable speed. *Proc IMechE, Part O: J Risk and Reliability* 2009; 223(1): 41–50.
- Tang B, Liu W and Song T. Wind turbine fault diagnosis based on Morlet wavelet transformation and Wigner-Ville distribution. *Renew Energ* 2010; 35(12): 2862–2866.

13. Feng Z, Liang M, Zhang Y, et al. Fault diagnosis for wind turbine planetary gearboxes via demodulation analysis based on ensemble empirical mode decomposition and energy separation. *Renew Energ* 2012; 47: 112–126.
14. Frei M and Osorio I. Intrinsic time-scale decomposition: time–frequency–energy analysis and real-time filtering of non-stationary signals. *P Roy Soc A: Math Phy* 2007; 463(2078): 321–342.
15. Huang N, Shen Z, Long S, et al. The empirical mode decomposition and the Hilbert spectrum for nonlinear and non-stationary time series analysis. *P Roy Soc A: Math Phy* 1998; 454(1971): 903–995.
16. Wu Z and Huang N. Ensemble empirical mode decomposition: a noise assisted data analysis method. *Adv Adapt Data Anal* 2009; 1(1): 1–41.
17. An X, Jiang D, Liu C, et al. Wind farm power prediction based on wavelet decomposition and chaotic time series. *Expert Syst Appl* 2011; 38(9): 11280–11285.
18. Übeyli E. Least squares support vector machine employing model-based methods coefficients for analysis of EEG signals. *Expert Syst Appl* 2010; 37(1): 233–239.
19. An S, Liu W and Venkatesh S. Fast cross-validation algorithms for least squares support vector machine and kernel ridge regression. *Pattern Recogn* 2007; 40(8): 2154–2162.
20. Li J, Liu H, Yao X, et al. Structure–activity relationship study of oxindole-based inhibitors of cyclin-dependent kinases based on least-squares support vector machines. *Anal Chim Acta* 2007; 581(2): 333–342.
21. Adankon M and Cheriet M. Model selection for the LS-SVM. Application to handwriting recognition. *Pattern Recogn* 2009; 42(12): 3264–3270.